

Frequency Reserve Management in Isolated Industrial Systems Dominated by **Constant Power Loads**

Gangavaram Thanuj¹

¹PG student/Dept. of EPS, PVKK Institute of Technology, Andhra Pradesh,India.

Abstract - This article explores the application of interconnected synchronous system requirements for frequency containment reserves (FCR) in isolated industrial grids. These grids typically rely on turbogenerators as the main energy source, have a high penetration of wind energy, include energy storage systems, and feature constant power loads connected through power electronic converters. Building on the recent Nordic FCRI requirements for islanded operation, we propose an extension that enables prioritization among different reserve providers based on specific grid

A complex isolated industrial grid is selected as a case study to evaluate this approach. The grid's stability is analyzed using eigenvalues and participation factors, taking into account the negative effects of constant power loads. The study shows that allocating reserves to faster, converter-interfaced storage devices and loads improves overall system stability and allows turbogenerators to operate under more constant loading conditions.

The results are validated through **computer simulations** in DIgSILENT PowerFactory and laboratory powerhardware-in-the-loop experiments, which compare the proposed approach to standard droop control methods. Furthermore, the **simulation models** developed for this made publicly available study are reproducibility.

Key Words: Power system control, frequency regulation, industrial power system management, energy storage systems, system stability, DC-AC power conversion.

1.INTRODUCTION

The petroleum sector contributes significantly to greenhouse gas (GHG) emissions in many countries, while also being a key driver of socio-economic development. For example, about 20% of Norway's total GHG emissions originate from single-cycle gas turbines operating in oil and gas (O&G) fields on the Norwegian Continental Shelf (NCS) [1]. Substantial emissions from offshore O&G operations are also reported in countries such as the United Kingdom [2] and the Netherlands [3].

To reduce these emissions, a floating wind farm (WF) consisting of eleven wind turbines (WTs) connected to two isolated O&G platforms in the North Sea has recently been commissioned [4], [5]. Such isolated industrial systems

pose several challenges in design, control, and operation, including instabilities caused by constant power loads and the effects of active power imbalances. Addressing these issues from the early design stage may require adapting the control strategies of generation units and optimizing the use of existing assets. The challenges of balancing excess or insufficient wind power in isolated O&G platforms have been explored in [6], [7], [8].

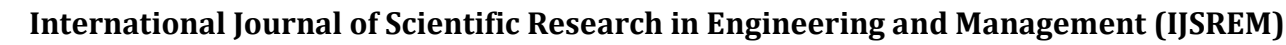
ISSN: 2582-3930

To mitigate the variability of wind power in offshore applications, energy storage systems (ESSs) have been studied in both centralized [9], [10], [11] and distributed [12] configurations. For example, the operation of a platform's water injection system as a flexible load in combination with wind power has been analyzed in [13], [14], [15], [16].

Two critical operational aspects in such systems are frequency control and the continuous compensation of imbalances between generation and consumption. These are typically managed by activating distributed power reserves in a hierarchical manner. Primary reserves use droop-based frequency control, responding automatically to power imbalances and limiting frequency deviations within seconds. Secondary reserves operate under the grid's automatic generation control (AGC), restoring frequency to its nominal value within seconds to minutes following imbalances [17]. In the European context, primary reserves are referred to as frequency containment reserves (FCR) and are coordinated nationally by transmission system operators (TSOs) [18].

Recently, three types of frequency containment reserves (FCR) have been defined for the Nordic synchronous area, which includes the power grids of Finland, Sweden, Norway, and eastern Denmark [19]. These are: normal operation frequency containment reserves (FCRN), large disturbance frequency containment reserves (FCRD), and islanded operation frequency containment reserves (FCRI). While FCRN and FCRD work together in the interconnected system, FCRI are a simplified version of FCRN and FCRD, activated only during islanding events. A single provider can supply any of these reserves, depending on technical qualification and grid operating conditions. Markets managed by national transmission system operators (TSOs) are expected to coordinate the availability of these three types of FCR in the Nordic area [20], [21], [22].

FCRN are active when the grid frequency remains within a **specified band** around the rated value. If the frequency moves outside this band, FCRN saturate, and FCRD are triggered. This frequency band is defined by the TSO and





SJIF Rating: 8.586

ISSN: 2582-3930

is common to the entire grid. In interconnected operation, an FCR provider may have **two distinct slopes** in its **power-frequency droop characteristic**—one for FCRN and another for FCRD [19]. For larger frequency deviations or high rates of change in frequency, as defined by the TSO, the provider switches to **FCRI mode**, adopting a **single slope** for the droop characteristic [23].

In **offshore isolated industrial grids**, active power sharing among generators typically follows one of three strategies [24], [25], [26], [27]:

- 1. All units operate in **isochronous mode**.
- 2. One unit operates in isochronous mode, while the others operate in **droop control**.
- 3. All units operate in droop control with a centralized secondary frequency controller in the grid's power management system (PMS).

The first strategy requires a fast communication link between generators, either through analog hardwired connections or serial communication. If this link fails, the system defaults to droop control strategies, which are similar to **FCRI operation** in the Nordic synchronous area. It is important to note that, although isolated offshore generators operate analogously to FCRI, they are not required to comply with TSO-defined grid codes. In this article, we propose an expansion of the Nordic synchronous area FCRI concept, along with a theoretical framework for analyzing the distribution of primary power reserves among multiple providers. The original FCRI's single-slope power-frequency droop is extended into a **segmented droop**, with distinct regions for normal operation and large disturbance events. To the authors' knowledge, this expanded FCRI concept has not been applied in the offshore industry [24], [25], [26], nor in studies of isolated offshore O&G platforms connected to wind farms (WFs) with or without energy storage systems (ESSs) [7], [8], [10], [11], [28], [29], [30], and it has not been examined with inertial support provided by wind turbines [8]. Additionally, this concept has not been employed in studies of power-intensive land-based isolated grids with hydro, diesel, or coal-based synchronous generation balancing intermittent wind or photovoltaic (PV) generation [31], [32], nor in the literature on AC microgrids [33], [34], [35].

This study investigates the **stability and performance improvements** achieved through the **coordinated distribution of primary reserves** based on the expanded FCRI concept, using a **representative O&G installation** as a case study. Analyses are performed with **numerical simulations** in DIgSILENT PowerFactory 2020 SP2A and **experimental validation**. First, the impact of varying contributions from **traditional synchronous generators** and **converter-interfaced devices** on the system's

eigenvalues is evaluated. Subsequently, experimental results from real-time system (RTS) and power-hardware-in-the-loop (PHIL) tests are presented, demonstrating their effectiveness for analyzing and validating devices and controls in isolated grids [36]. As shown in Section VII, the expanded FCRI provides improved performance compared to conventional droop control, particularly in terms of frequency regulation and nadir.

The main contributions of this article are as follows:

- 1. It introduces an **expanded Nordic FCRI concept** and demonstrates, through simulations and experimental tests, the advantages of **replacing slower turbogenerators (GTs)** with **faster converter-interfaced ESSs** as the primary providers of power reserves. This substitution results in a **non-critical reduction in damping** of oscillation modes associated with frequency measurement transducers and controllers of **constant power devices**.
- 2. It considers the **negative effects of constant power loads (CPLs)** in the electrical grid, a factor often overlooked in studies of power-intensive isolated grids.
- 3. It compares the expanded FCRI approach with state-of-the-art industry control strategies, providing valuable insights for applying this concept in complex islanding scenarios involving traditional synchronous generation, high participation of intermittent renewable energy sources (RESs), and ESSs.

The structure of this article is as follows: Section II introduces the expanded FCRI concept and discusses issues arising from constant power loads (CPLs). Section III explains the sharing and coordination of power reserves in an isolated grid. In Section IV, a theoretical approach for the expanded FCRI concept is presented through modeling and stability analysis. Section V describes the case study, while Section VI provides a detailed stability assessment. Section VII presents the experimental validation using laboratory power-hardware-in-the-loop (PHIL) tests. Section VIII compares the proposed concept with a state-of-the-art offshore industry control strategy, followed

by a discussion in Section IX, and concluding remarks in Section X.

SJIF Rating: 8.586

ISSN: 2582-3930

2. Frequency Containment Reserves for Operation in Isolated Grids Dominated by Constant Power Loads

Both large interconnected systems and isolated grids face significant challenges due to the growing penetration of intermittent renewable energy sources (RESs). In the Nordic synchronous area, primary reserve providers are required to maintain two sets of parameters: one for islanded operation and another for interconnected operation. During an islanding event, a reserve provider must switch to FCRI mode and adopt a single-slope power-frequency droop characteristic [23], as illustrated in Fig. 1.

In this context, this article proposes an expansion of the Nordic FCRI concept, transforming the original single-slope droop into a segmented droop with distinct regions for normal operation and large disturbance events, as shown in Fig. 2. This expanded concept is applied to a case study representing an O&G platform connected to a wind farm (WF) and equipped with an energy storage system (ESS). For simplicity, the normal isolated operation reserves are denoted as FCRN, and the large disturbance reserves for isolated operation are denoted as FCRD. These FCRN and FCRD for isolated grids are analogous to the corresponding reserves defined for interconnected operation in [19].

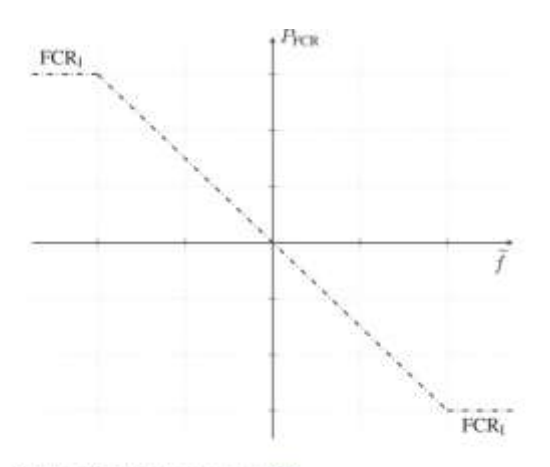


Fig. 1. Original FCR₁ characteristic [23].

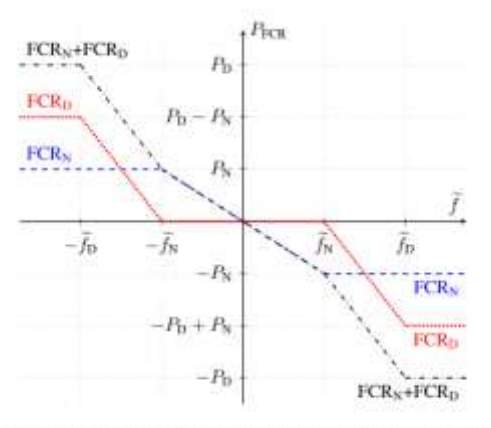


Fig. 2. Proposed expanded FCR₁ characteristic of the system, adapted from the FCR_{N+D} for interconnected operation defined by [19].

The **expanded FCRI characteristic** of the system is illustrated in Fig. 2. The boundary fN_NN between the **FCRN** and **FCRD** activation regions is defined based on the deviation of the measured AC frequency f from its nominal value fn_nn , i.e., $\Delta f = f - fn \Delta f = f - f - f \Delta f = f - f$. The **FCRN** are active while **FCRD** remain inactive when $|\Delta f| \le fN |\Delta f| \le fN |\Delta f| \le fN$. For the **Nordic interconnected grid**, fNf_NfN is set to **0.1 Hz (0.2%)** [19].

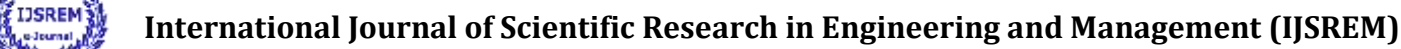
However, **isolated grids** typically experience larger **relative power imbalances** and more severe **frequency disturbances** than continental or national grids. For example, recommended practices for electrical power generation in **merchant**, **commercial**, **and naval vessels** [37] specify a tolerance of $\pm 3\%$ for the "maximum permitted departure from nominal frequency during normal operation, excluding transient and cyclic variations." Accordingly, a value between 0.2% and 3% will be used for fNf NfN in **Sections VII and VIII**.

A system is considered to be under a **large disturbance** when $|\Delta f| > fN|\Delta f| > fN|\Delta f| > fN$. In this case, **FCRN** saturate at PNP_NPN, and **FCRD** are activated to maintain frequency stability.

B. Constant Power Loads

Wind turbines (WTs) and solar PV panels can be considered constant power sources (CPSs) because their controllers typically operate in maximum power point tracking (MPPT) mode, which maintains optimal power output for a given wind speed or solar irradiation [38]. Storage devices (SDs) connected to a common ESS DC link, as studied in [9], [10], can also function as constant power loads (CPLs) or CPSs. Isolated industrial grids often supply significant CPLs, such as variable frequency drives [13], [39].

Although CPLs and CPSs are known to cause instabilities in DC microgrids [40], [41] and AC microgrids [42],



IJSREM 1

Volume: 09 Issue: 10 | Oct - 2025 SJIF Rating: 8.586 ISSN: 2582-3930

[43], studies on integrating wind power supported by ESSs and converter-interfaced flexible loads (FLX) [9], [10], or only by ESSs [11], [28], frequently model the total electrical load of an isolated O&G platform as constant impedance loads (CZLs).

Power electronics-focused studies on CPLs in microgrids [44], [45] tend to emphasize converter stability rather than grid frequency control or overall grid stability. When combined with power electronic converters (PECs), CPLs and CPSs can introduce new instability phenomena in both microgrids and large interconnected grids [36], [46]. Modern Type 4 WTs [47], solar PV farms, ESSs, and certain load types are all connected via full-power PECs. Therefore, converter-driven instabilities should not be overlooked when integrating this equipment into isolated grids.

III. SHARING AND COORDINATION OF PRIMARY AND SECONDARY RESERVES

The **stochastic nature of wind** can lead to more frequent start-stop operations and highly variable load profiles for the gas turbines (GTs) of an O&G platform connected to a wind farm (WF). This results in increased mechanical wear, higher unintended nitrogen oxides (NOx) emissions, and overall degradation of power quality and frequency stability [48], [49]. coordination strategies that prioritize converterinterfaced loads (CILs) and energy storage systems (ESSs) over GTs as the main sources of power for fast frequency control are essential for the effective integration of wind power into offshore O&G facilities. In this section, a hierarchical frequency control structure is presented that enables such prioritization while incorporating the extended FCRI concept.

A. Secondary Reserves

Fig. 3 illustrates the frequency control structure of the study case's autonomous grid, in which reserve providers operate in a subordinate role under a centralized power management system (PMS). The secondary frequency controller, a component of the PMS, is responsible for correcting steady-state frequency errors in the isolated grid. It employs a proportional-integral (PI) regulator that responds to frequency deviations and generates the total secondary power reference PS*P_S^*PS*, which is distributed among two gas turbines (GTs) and a pair of fuel cell (FC) and electrolyzer (EL) units.

The measured and filtered power outputs of the FC and EL, denoted as PFCP_{FC}PFC and PELP_{EL}PEL, are **subtracted** from the secondary power reference sent to the GT governors, as shown in (1). Although not depicted in Fig. 3, the reserve providers have **individual limits** on their **rate of change of power**, and the GTs include an **additional input** for dynamic control.

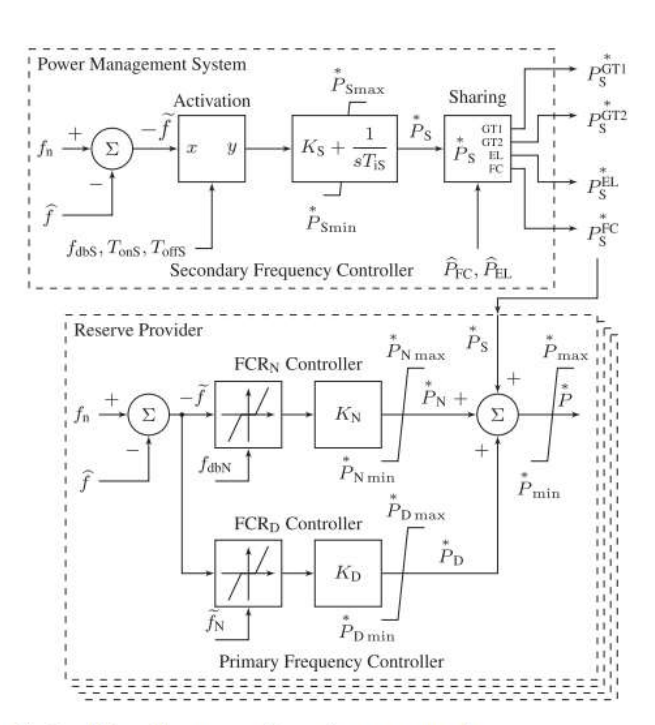


Fig. 3. Hierarchic structure of the ac frequency control.

B. Primary Reserves

Distributed primary frequency control is implemented locally at each reserve provider. All FCRN providers must be capable of delivering their allocated reserve power PNP_NPN in response to a frequency drop of fNf_NfN, and conversely, absorbing PNP_NPN for a frequency increase. For the entire system, this proportional response is referred to as regulating strength [19] or frequency bias [17]; in this article, it will be termed FCR gain or frequency-to-power gain.

The total **frequency-to-power characteristic** of the system combines the contributions of both **normal (FCRN)** and **large disturbance (FCRD)** reserves, as illustrated in Fig. 2. The **FCRD controllers** include a **dead band** of \pm fN\pm f_N \pm fN, ensuring that only the FCRN are active during **normal operation**, as shown in Fig. 3. It is important to note that the gains KNK_NKN and KDK_DKD do not need to be equal. Additionally, the **FCRN** saturate at PNP_NPN, and the **FCRD** are activated when $|f| > fN|f| > f_N|f| > fN$.

C. FCR Controllers

The power contribution of each FCR provider depends on the measured AC frequency fff. Each provider calculates the deviation from the rated frequency fnf_nfn, as shown in Fig. 3, and feeds the resulting $-\Delta f$ -\Delta f-\Delta f to two proportional controllers: one for FCRN and one for FCRD. Each controller has its own gain (K), limits (maximum and minimum), and a symmetric dead band (fdbNf_{dbN} fdbN and fNf_NfN). The FCRN power reference (PN*P_N^*PN*) and the FCRD power reference (PD*P_D^*PD*) are summed with the secondary power reference (PS*P S^*PS*), which is



SIIF Rating: 8.586

International Journal of Scien
Volume: 09 Issue: 10 | Oct - 2025

ISSN: 2582-3930

communicated to the providers by the **PMS**. The resulting **total power reference** (P*P^*P*) has independent **maximum and minimum limits**.

The PMS allocates a primary reserve quota to each provider based on a security assessment, considering grid operational conditions and load/RES forecasts. To qualify for a quota, a provider must respond symmetrically to both positive and negative frequency deviations and deliver the assigned reserve power PNP_NPN when $|\Delta f|=fN|$ Delta |f|=fN|Belta |f|=fN|Belt

It is important to note that the **transient response** of each FCR provider does **not depend on a fast communication link** with the PMS, as the **FCR control loops** are implemented **locally**, and rapid changes in power allocation are not anticipated.

D. Role of Dead Bands in FCR

The coordination of normal operation (FCRN) and large disturbance (FCRD) reserves is achieved using a dead-band block in the FCRD controllers, as illustrated in Fig. 3. The limit frequency fNf NfN is unique for the system and is known to all FCR providers. By setting the FCRD dead band to fNf NfN, it is ensured that large disturbance reserves are activated only after the FCRN saturated.The maximum and minimum limits $(PN* maxP N^{*}, text{max})PN*max$ $PN*minP N^{*},\text{text}\{min\}\}PN*min) of each FCRN$ provider are assumed to be symmetric, with absolute values equal to PNP NPN. In certain cases, a nonnegligible dead band fdbNf {dbN}fdbN may be required for proper operation of a specific FCRN provider. In such cases, calculating the gain KNK NKN using (2) may reduce the effective FCRN capacity. If a provider requires a small dead band for proper operation, the effects of the dead band can be compensated locally by calculating the **frequency-to-power gain** according to (4), without requiring intervention from the PMS.

IV. STABILITY ASSESSMENT WITH A ROTATING MASS MODEL

Converter-interfaced reserves respond significantly faster than traditional turbogenerators (GTs) [50]. The advantages of these faster responses can be initially evaluated using the classical rotating mass model [51], [52]. In this approach, the spinning reserves of the system (i.e., the GTs) are aggregated into a single rotating mass with moment of inertia JJJ. The turbines apply torque to increase the angular frequency ω\omegaω of the rotating mass, while the aggregated electrical loads exert torque to reduce ω\omegaω.

When **primary reserves** are supplied by traditional GTs, the **intrinsic delay** of the governor and turbine is on the order of **hundreds of milliseconds** [54]. In contrast, if the primary reserve is provided by an **ESS**, the delay is reduced by at least **one order of magnitude** [50]. As TTT in (9) approaches zero, the **transfer function** between power imbalance and system frequency approximates a **first-order low-pass filter**.

For normal operation of an isolated grid, allocating FCRN to ESS while leaving the GTs with only FCRD provides a two-fold advantage. First, the GTs can operate at more constant power, reducing mechanical wear. Second, the system exhibits reduced oscillations, even without implementing a virtual synchronous machine (VSM) scheme or derivative terms in the ESS reserves.

A. Multiple FCR Providers

The **power balance** in (7) can be expressed as (11) for a system with nnn **reserve providers**, each modeled as a **first-order low-pass filter (LPF)** with gains kik_iki and delays TiT_iTi , as described in (8). The resulting **transfer function G(s)G(s)G(s)** between power ppp and frequency fff becomes of order n+1n+1n+1, as shown in (12). A **constant power imbalance ppp** produces a **steady-state frequency deviation** that is **inversely proportional** to the sum of gains $k1k_1k1$ to knk_nkn and is **independent** of the system inertia or the providers' time delays. This is demonstrated in (13) using the **final value theorem** applied to G(s)p(s)G(s)p(s)G(s)p(s) when the imbalance p(s)p(s)p(s) is a step input of amplitude ppp.

However, the **inertia HHH**, delays TiT_iTi, and gains kik_iki influence the **location of the poles** of G(s)G(s)G(s) in the **complex plane**, thereby affecting the **damping** and **natural frequency** of the system's oscillatory modes. It is important to note that the **linearized rotating mass model**, which results in (9) and (12), **neglects the detailed dynamics** of the electrical grid. While a comprehensive **stability analysis** requires a more sophisticated model, this simplified approach provides **valuable insights** into the effects of system inertia, gains, and time delays. Additional details on conditions for **robust frequency stability** in power grids can be found in [55].

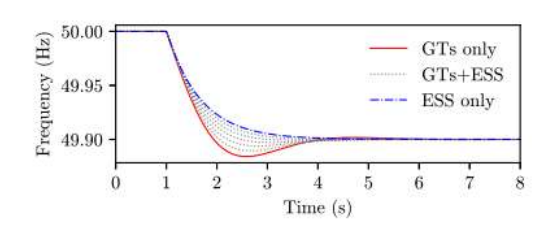


Fig. 4. Frequency during a step load of $1.2\,\mathrm{MW}$ with different sharing of FCR_N between ESS and GTs.

SJIF Rating: 8.586

ISSN: 2582-3930

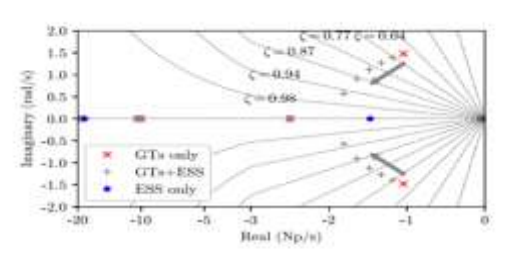


Fig. 5. Eigenvalues with linearized rotating mass model for a total gain of 12 MW/Hz and different sharing of FCR_N between ESS and GTs.

B. Modal Analysis

It is insightful to evaluate the **stability** of the study case using the **simplified model** described in (11) when the **FCR** is shared between **two GTs** and an **ESS**. For this purpose, the normalized **pFCR** is divided into **three components**: one for the ESS and two for the GTs. The **ESS component** is modeled as a **first-order LPF**, while the GT components use **two first-order LPFs in series** to represent the **fuel valve** and **turbine delays**. Model parameters are provided in **Table I**.

The total **power-to-frequency gain** of the FCR is set to KN=12 MW/HzK_N=12\\text{MW/Hz}KN=12 MW/Hz and is shared between the GTs and ESS. This gain is relatively high compared to the installed GT power of 88 MVA and the system load of 44 MW. For large interconnected grids in **North America**, typical gains range around **10% of peak demand in W/Hz** [17].

Figures 4 and 5 show, respectively, the frequency response following a 1.2 MW step load and the system eigenvalues obtained using MATLAB Simulink R2018a for seven different FCR sharing configurations listed in Table II. The model and dataset are publicly available at [56]. The frequency nadir—the minimum value reached after the step—is significantly improved when the primary reserves are shifted from the slower GTs to the faster ESS.

V. STUDY CASE: AN ISOLATED INDUSTRIAL GRID

The study case considered in this article is based on an existing O&G platform in the North Sea, which operates isolated from the mainland. Under normal conditions, the platform is powered by two 35.2 MW aero-derivative single-cycle GTs. A techno-economic study [49] suggested that connecting the platform to a 12 MW floating offshore wind farm (WF) could reduce annual CO₂ emissions by approximately 30%. Achieving this reduction, however, requires the installation of a centralized hybrid ESS, consisting of 4 MW proton exchange membrane (PEM) fuel cells and 6 MW PEM electrolyzers.

A prospective scenario in [9] considered three 4 MW WTs for sizing the platform's hybrid ESS, and this scenario was also employed in [10] and [57]. Figure 6 shows the single-line diagram of the study case. The platform has an average electrical load of 44 MW, which cannot be fully supplied by a single 35.2 MW GT. Moreover, the thermal load of industrial processes [13] requires at least one GT to operate at all times. For safety reasons, the scenario in [9], [10], and [57] assumed that both GTs operate simultaneously, even when the WF is producing at full capacity. This assumption is maintained in the present study to allow reuse of the previously established scenario.

The platform loads are divided into three groups in Fig. 6. The first group represents the water injection system, whose variable frequency drives (VFDs) can operate as flexible loads (FLX) providing primary frequency control reserves. For simplification, the entire water injection system is modeled as a single 8.5 MVA active-front-end PEC. The second group consists of 26 MW of constant power loads (CPLs), which are modeled as instantaneous constant power consumers, i.e., without associated delays. The third group includes 11 MW of constant impedance loads (CZLs). Both CPLs and CZLs can be modified in steps to test the dynamic behavior of the model.

The FLX are represented as a single ideal controlled current source feeding a DC link, where the current output depends on the power demand of the flexible loads.

VI. DETAILED STABILITY ASSESSMENT

The **mechanical rotating mass model**, which leads to the transfer functions in (9) and (12),

IEEE TRANSACTIONS ON POWER SYSTEMS, VOL. 39, NO. 2, MARCH 2024

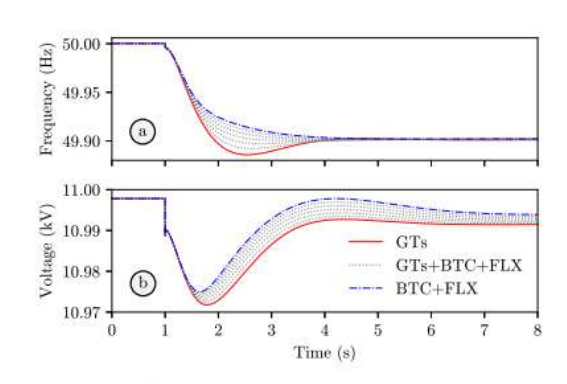
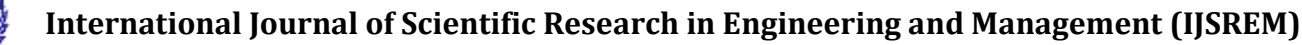


Fig. 8. Voltage and frequency at the main busbar during a step load of 1.2 MW.





SJIF Rating: 8.586

connected to the high-voltage side of the ESSTR, while the DC grid emulator functions as a controlled current source, supplying the DC link of the ESS with the net current from the ESDs. The scaling details for the hardware under test are provided in Table III.

ISSN: 2582-3930

Three experimental test cases were designed:

- Case 1 FCRN supplied solely by the GTs;
- Case 2 FCRN shared between the BTC and GTs;
- Case 3 FCRN shared between the BTC and FLX.

In all cases, the total available FCRN is PN = 3 MW, while FCRD is provided only by the GTs. The boundary between normal and large disturbance operation is set at fN = 1 Hz, and the total FCRD gain is 6 MW/Hz, concentrated entirely in the GTs. The chosen value of fN corresponds to 2% of the rated system frequency, which exceeds the 0.2% limit typically required for the Nordic synchronous area [19] but remains below...

Figure 8(a) illustrates seven instances of frequency variations caused by a **1.2 MW step load**. The frequency was measured at the platform's **main busbar** using a **phase-locked loop (PLL)** [66]. Each of the seven cases corresponds to a different **FCRN sharing configuration**, as listed in Table II. The step load is applied at **t** = **1 s**, and within the following **4 seconds**, the frequency stabilizes at **49.9 Hz**.

The solid red curve represents the response when the GTs are the sole FCRN providers, reaching a minimum frequency (nadir) of 49.886 Hz. The dotted gray curves correspond to cases where the FCRN is shared among GTs, the battery converter (BTC), and the flexible loads (FLX). The dash-dotted blue curve shows the response when only BTC and FLX provide FCRN. From a frequency control perspective, the system exhibits improved stability as the primary reserves shift toward the faster BTC and FLX, resulting in a higher nadir.

Comparing the results in Fig. 8(a) with the simplified rotating mass model in Fig. 4, the overall trends are similar. However, the detailed **DIGSILENT** PowerFactory 2020 SP2A simulations reveal additional complex interactions that can influence grid stability. For instance, the main busbar voltage response in Fig. 8(b) is slightly less damped. Therefore, the voltage control dynamics of the active front-end converters (ESSGC and FLXGC) should be considered in any comprehensive stability analysis.

Hg 12. Whiteness of the Pills, may had with the Propulation work jumps and an 100 had been subtract of the Pills.

VIII. EXTENDED FCRI VERSUS INDUSTRY STATE-OF-THE-ART

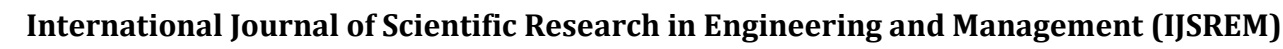
In this section, the **extended FCRI concept** is benchmarked against the **industry-standard droop control** with a centralized secondary frequency controller. **Case 3** from Section VII is selected for this comparison. The dead bands for the FCRN providers are set to **10 mHz**. In the traditional droop scenario, the total frequency-to-power gain of **3 MW/Hz** is distributed among the primary reserve providers as follows: **0.5 MW/Hz** for each GT, **1 MW/Hz** for the BTC, and the remaining **1 MW/Hz** for the FLX. The effects of wind turbulence on the WTs are also considered, as detailed in [9], [56].

VII. VALIDATION OF THE POWER HARDWARE IN THE LOOP TEST SETUP

In this section, the **PowerFactory model** described in Section VI is compared with a **real-time simulator (RTS) model** [68] using a **scaled-down PHIL test setup** at the **National Smart Grid Laboratory of NTNU**, as shown in Fig. 10. This test setup is also utilized in Section VIII to compare the performance of the **proposed extended FCRI concept** against a **state-of-the-art control strategy** employed in power-intensive isolated industrial grids. The **hardware under test** includes the **ESSGC**, the **dc link capacitance**, and an **inductive-capacitive-inductive** (LCL) filter.

11. Scaled-down PHIL Test Rig
The hardware components under test, indicated with a
dashed rectangle in Fig. 6, include the filter and associated
devices. Their connections to the AC and DC grid
emulators [69] are shown in Fig. 11. The AC grid
emulator operates as a controlled voltage source and is

Fig. 13 presents a comparison of system performance between the traditional droop method and the FCRN+D implementation of Case 3. At t = 10 s, a sudden loss of 11 MW in wind power occurs (Fig. 13(c)). The PI regulator of the secondary power controller responds immediately to



IJSREM Second

Volume: 09 Issue: 10 | Oct - 2025 SJIF Rating: 8.586 ISSN: 2582-3930

the frequency deviation, adjusting the secondary power reference, which in turn triggers the response of the **ELC** and **FCC** units (Fig. 13(f)). The difference between the required...

The difference between the required secondary power and the **measured power delivered** by the ELC and FCC is forwarded as a reference to the GTs, as specified in (1). Consequently, the mechanical power supplied by the turbines to the synchronous generators (Fig. 13(d)) reflects both the droop response and the secondary power contribution. In FCRN+D Case 3, the BTC and FLX are prioritized as primary providers during normal operation. The 11 MW loss in wind generation causes these FCRN providers to reach saturation (Fig. 13(b) and (e)) when the system frequency drops below 49 Hz (Fig. 13(a)). Any potential power deficit resulting from this saturation is automatically compensated by the activation of the FCRD from the GTs. By properly defining f_n and calculating the gains K_n and K D using (2) and (3), the framework ensures that any saturation of FCRN providers is reliably mitigated through the FCRD activation.

IX. DISCUSSION AND FUTURE WORK

The main advantage of the **extended FCRI concept** compared to the traditional droop method is the **flexibility** in selecting which units provide normal operation reserves and which provide large disturbance reserves. Furthermore, the proposed concept allows assigning **different frequency-to-power gains** for each operating condition in isolated grids. It is important to note that the same provider can participate in both reserve types depending on technical or economic considerations.

The provision of primary reserves by faster ESS and FLX reduces the frequency control burden on slower GTs, resulting in lower wear and tear of turbine governors, reduced NOx and CO₂ emissions, and improved overall power quality on the platform. Although higher participation of faster reserves results in a more damped frequency response after sudden load changes, there is a non-critical increase in oscillations at the main busbar voltage. Therefore, interactions between the GT excitation system and the reactive power control of ESSGC require careful attention. Additionally, tuning of the ESS and FLX frequency measurement devices must be carefully performed, as oscillation modes associated with these devices can move toward less-damped regions of the complex plane when their contributions increase.

Nevertheless, eigenvalue analysis and dynamic simulations in PowerFactory, as well as results from the PHIL test setup, indicate that the benefits—from a grid stability perspective—outweigh the disadvantages of increasing the share of converter-interfaced FCRN reserves in primary frequency control for isolated grids.

As the total allocated reserve power is maintained by the **PMS**, a higher participation of the **battery** in the primary frequency control contributes to a more **stable and responsive system**.

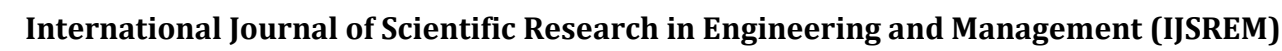
Notwithstanding, there exists a series of modes with damping ratio ζ close to or lower than 0.5, which are associated with constant power devices such as the **fuel cell, electrolyzer, and WTs**. Different tuning strategies for the controllers of these devices influence the location of these oscillation modes in the **complex plane**. However, an assessment of such tuning strategies is considered **outside** the **scope of this article** and will be addressed in future work.

There are a few discrepancies between the results obtained with the PHIL setup and the PowerFactory simulations. The most noticeable discrepancy is in the FCC power, which is due to higher losses in the scaled-down hardware devices (denoted by ESSGC, ESSLac, and ESSTR in Figs. 6 and 11) that are not present in the PowerFactory simulations. Normalized resistive losses in laboratory equipment such as transformers, reactors, and converters tend to be higher than the normalized losses in their full-scale counterparts. A compromise between reducing losses and matching reactance and capacitance values in per unit (pu) has to be made for a scaled-down PHIL test. This topic is addressed in more detail in [70].

X. CONCLUSION

In this article, the Nordic synchronous system concept of **islanded operation frequency containment reserves** (FCRI) was expanded and subdivided into two categories. This strategy of categorized FCRI was applied to the study case of an **isolated complex industrial system** which is fed by traditional GTs and by a WF, is dominated by CPLs, equipped with fast flexible CILs, and supported by an ESS.

The analyses performed in this work took into consideration the detrimental effects of the CPLs and demonstrated that the overall stability of the system increased by shifting the **primary power reserves** from the slow GTs to the fast ESS and CILs. This also allowed the GTs of the study case to operate at a **more constant power**, which has the potential to reduce **wear and tear in the**



SJIF Rating: 8.586

ISSN: 2582-3930

turbine governors. While the reduction in the damping of oscillation modes associated with the CPLs and the PECs was not critical, the oscillation mode associated with the slow turbine governors was considerably damped when ESS and CIL reserves were prioritized.

The results of this article were supported by **computer simulations**, made publicly available, and **PHIL tests**. They demonstrate the versatility of the expanded FCRI concept for **coordinating fast primary power reserves** in autonomous grids with increased participation of **non-synchronous intermittent RESs**.

REFERENCES

- [1]"Hywind Tampen PUD del II-Konsekvensutredning," Equinor, Oslo, Norway, Impact Assessment Report PL050 - PL057 - PL089, Mar. 2019
- [2] "North sea transition deal," Dept. Business, Energy Ind. Strategy, London, U. K., Report NSTD, Mar. 2021.
- [3] A. S. Tamez and S. Dellaert, "Decarbonisation options for the dutch offshore natural gas industry" PBL Netherlands Environ. Assessment Agency and TNO Energy Transition, Hague, The Netherland, Report PBL 416, 2020.
- [4] "Hywind Tampen PUD del II-Konsekvensutredning," Equinor, Oslo, Norway, Impact Assessment Report PL050 PL057 PL089, Mar. 2019.
- [5] "First Power from Hywind Tampen," Equinor, Oslo, Norway, Press release, Nov. 2022.
- [6] H. G. Svendsen, M. Hadiya, E. V. Øyslebø, and K. Uhlen, "Integration of offshore wind farm with multiple oil and gas platforms," in Proc. IEEE Trondheim PowerTech, 2011, pp. 1–3.
- [7] A. R. Ardal, T. Undeland, and K. Sharifabadi, "Voltage and frequency ocontrol in offshore wind turbines connected to isolated oil platform power systems," Energy Procedia, vol. 24, pp. 229–236, Jan. 2012.
- [8] A. R. Ardal, K. Sharifabadi, O. Bergvoll, and V. Berge, "Challenges with "integration and operation of offshore oil & gas platforms connected to an offshore wind power plant," in Proc. IEEE Petroleum Chem. Ind. Conf. Eur., 2014, pp. 1–9.

- [9] E. Alves, D. d. S. Mota, and E. Tedeschi, "Sizing of hybrid energy storage systems for inertial and primary frequency control," Front. Energy Res., vol. 9, May 2021, Art. no. 649200.
- [10] D. d. S. Mota, E. F. Alves, S. Sanchez-Acevedo, H. G. Svendsen, and E. Tedeschi, "Offshore wind farms and isolated oil and gas platforms: Perspectives and possibilities," in Proc. 41st Int. Conf. Ocean, Offshore Arctic Eng.2022, Art. no. V010T11A048.
- [11] T. J. Zhong, I. L. Hong Lim, and J. Yang, "Energy management strategy designed for offshore oil rig with offshore wind," in Proc. IEEE 16th Int. Conf. Compat., Power Electron., Power Eng., 2022, pp. 1–6.
- [12] T. Zhou and B. Francois, "Energy management and power control of a hybrid active wind generator for distributed power generation and grid integration," IEEE Trans. Ind. Electron., vol. 58, no. 1, pp. 95–104, Jan. 2011.
- [13] H. Devold, Oil and Gas Production Handbook: An Introduction to Oil and Gas Production, Transport, Refining and Petrochemical Industry, 3rd ed. Oslo, Norway.
- [14] S. Sanchez, E. Tedeschi, J. Silva, M. Jafar, and A. Marichalar, "Smart load management of water injection systems in offshore oil and gas platforms integrating wind power," IET Renewable Power Gener., vol. 11, no. 9, pp. 1153–1162, Jul. 2017.
- [15] "WIN WIN Joint Industry Project: Wind-Powered Waterr Injection," DNV GL AS, Høvik, Norway, May 2019.

BIOGRAPHIES



Name - Gangavaram Thanuj